{Ni4} Cubanes from enantiomerically pure 2-(1-hydroxyethyl)pyridine ligands: supramolecular chirality†

Julia Mayans,[a] Angeliki A. Athanasopoulou,[b] Amy Trinh Pham,b Mercè Font-Bardia,[c] Eleni C. Mazarakioti,[b] Melanie Pilkington, *[b] Theocharis C. Stamatatos *‡[b] and Albert Escuer *[a]

a Departament de Química Inorgànica i Orgànica, Secció Inorgànica and Institute of Nanoscience (IN2UB) and Nanotechnology, Universitat de Barcelona, Marti i Franques 1-11, Barcelona-08028, Spain
b Department of Chemistry, 1812 Sir Isaac Brock Way, Brock University, L2S3A1 St. Catharines, Ontario, Canada. E-mail: mpilkington@brocku.ca
c Departament de Mineralogia, Cristal·lografia i Dipòsits Minerals and Unitat de Difracció de R-X, Centre Científic i Tecnològic de la Universitat de Barcelona (CCiTUB), Universitat de Barcelona, Solé i Sabarís 1-3, 08028 Barcelona, Spain

albert.escuer@qi.ub.es.(Albert Escuer)

ABSTRACT:

Homometallic {NiII
4} cubane-like clusters with a rare chiral core have been prepared via the employment of enantiomerically pure 2-(1-hydroxyethyl)pyridine (Hmpm). Comparison with the achiral cubanes derived from the related 2-pyridinemethanol (Hpym) ligand reveals drastic structural changes as a consequence of the transfer of chirality from the ligands to the whole structure. Their magnetic properties have Homometallic {NiII
4} cubane-like clusters with a rare chiral core have been prepared via the employment of enantiomerically pure 2-(1-hydroxyethyl)pyridine (Hmpm). Comparison with the achiral cubanes derived from the related 2-pyridinemethanol (Hpym) ligand reveals drastic structural changes as a consequence of the transfer of chirality from the ligands to the whole structure. Their magnetic properties have been related to the structural features of their cubane-type cores.been related to the structural features of their cubane-type cores.

INTRODUCTION

The search for new polynuclear metal complexes (or metal clusters) is driven by a number of considerations, the most crucial of which is the selection of the bridging/chelating organic ligand(s). The chemical, structural and electronic nature of these groups can undoubtedly affect the properties of the resulting molecular species, leading to compounds with interesting supramolecular, magnetic, optical, conductive, chiral and catalytic properties, to name a few. To this end, there is a continuous need for new multifunctional organic chelates that afford metal clusters with more than one physical and/or chemical property.

2-Pyridinemethanol (Hpym, Scheme 1) is a classical chelating/ bridging ligand employed in coordination chemistry for which around 500 entries corresponding to transition or lanthanide complexes can be found in the CCDC database. In contrast, the chemistry of the related chiral ligand 2-(1-hydroxyethyl) pyridine (Hmpm, Scheme 1) remains practically unexplored and only a few organometallic derivatives,1 polyoxometallates2 and coordination complexes3 have been reported to date. Hmpm is a very interesting ligand because in addition to excellent donor properties that can be inferred from its similarity with Hpym, the employment of enantiomerically pure (R)- or (S)-Hmpm opens up the way to incorporate additional properties into the resulting clusters.

The employment of chiral ligands promotes new optical properties that can be spectroscopically studied by means of electronic, infrared or Raman circular dichroism (absorption) or circular polarize luminescence (emission, in particular more favourably related to lanthanide systems), as well as chiral supramolecular effects that become particularly important in molecular recognition processes or enantioselective catalysis.4 In cluster chemistry, the chiral information introduced by the ligands is transferred to the system at different levels inducing Δ or Λ conformation on the octahedral environment of the cations, generating chiral cores or chiral supramolecular networks that cannot be obtained from racemic mixtures of the starting ligands or achiral donors.5

In this paper we report the first derivatives of Hmpm in nickel chemistry with the formula [Ni4(R-mpm)4(MeCOO)4]·6.5H2O 1R·6.5H2O, [Ni4(S-mpm)4(MeCOO)4]·2.5H2O·0.5H2O 1S·2.5H2O·0.5H2O [Ni4(R-mpm)4(t-butCOO)4]·H2O 2R·H2O and [Ni4(S-mpm)4-(t-butCOO)4] 2S that have been structurally characterized by X-ray diffraction and further studied by electronic circular dichroism (ECD) and magnetic susceptibility measurements. The new complexes are the first cubane derivatives from Hmpm and provide exceptional examples of the transfer of chirality from the ligands to the cluster core in homometallic cubanes

EXPERIMENTAL

Materials and methods

IR spectra (4000–400 cm−1) were recorded on a Bruker IFS-125 FT-IR spectrometer with samples prepared as KBr pellets. Variable-temperature magnetic studies were performed using a MPMS5 Quantum Design magnetometer operating at 0.03 T in the 300–2.0 K range. Diamagnetic corrections were applied to the observed paramagnetic susceptibility using Pascal constants. The quality factor was parametrized as R = (χMTexp −χMTcalc)2/(χMTexp)2. ECD spectra in the solid-state and solution (methanol or dichloromethane) were recorded on a Jasco-815 spectropolarimeter.

(R)- and (S)-2-(1-hydroxyethyl)pyridine were purchased from TCI Chemicals and used without further purification. The syntheses were performed in open air in reagent grade materials and solvents. Only well-formed crystals were employed for the performance of the reported measurements.

Single-crystal X-ray crystallography

Green prism-like specimens of dimensions 0.095 mm × 0.125 mm × 0.289 mm (1R·6.5H2O) and 0.111 mm × 0.201 mm × 0.202 mm (1S·2.5H2O·0.5H2O) were used for the X-ray crystallographic analysis. The X-ray intensity data were measured on a D8 Venture system equipped with a multilayer monochromator and a Mo microfocus (λ = 0.71073 Å). The frames were integrated with the Bruker SAINT software package using a narrow-frame algorithm. The final cell constants were based upon the refinement of the XYZ-centroids of reflections above 20σ(I). The structures were solved and refined using the Bruker SHELXTL software package.6 The compounds 1R·6.5H2O and 1S·2.5H2O·0.5H2O are not enantiomers in its strict sense, because they crystallize in different space groups (C2221 and P21212 respectively). This difference is due to the different number of crystallization solvent molecules that allow different space groups with two quasi identical cell parameters and a double size for the third one. On the other hand, the arrangement of the clusters in the network, topology of the clusters and their bond parameters follows the mirror-image that must be expected for a normal pair of enantiomers.

Single crystals of dimensions 0.20 mm × 0.15 mm × 0.05 mm for complex 2R·H2O were mounted on a Bruker APEX-II CCD diffractometer equipped with a CCD area detector and an Oxford Cryoflex low temperature device. Cell refinement and data-reduction were carried out using SAINT. The structure was solved by direct methods in SHELXS-97 and refined using SHELXL-2014 in the Bruker SHELXTL suite.6 The estimated electron density from the SQUEEZE process suggests that there is at least one water molecule associated with the formula unit of the cluster, consistent with the elemental analysis data. Cell parameters (monoclinic, a = 12.45 Å, b = 20.45 Å, c = 12.02 Å, α = 90°, β = 114.35°, γ = 90°, V = 2789 Å3) for 2S confirm its isostructurality with 2R.

Details of crystal data, collection and refinement for 1R, 1S and 2R are summarized in ESI, Table S1.† [Ni4(R-mpm)4(MeCOO)4]·6.5H2O (1R) and [Ni4(Smpm) 4(MeCOO)4]·2.5MeOH·0.5H2O (1S).

Ni(MeCOO)2 (0.5 mmol, 0.046 g) was dissolved in MeOH (10 mL) and the ligand S- or R-Hmpm (0.5

mmol, 0.62 g) was dissolved in MeCN (5 mL). The solutions were mixed, and the resulting green solution was stirred for four hours. The solution was then filtered and left to crystallize in a closed vial with a slow diffusion of diethylether. After two weeks, green crystals, adequate for X-ray diffraction were collected. The yield is around 40% of well-formed crystals. Anal. calcd for C36H57N4Ni4O18.5 (1R·6.5H2O): C, 40.16; H, 5.34; N, 5.20%. Found: C, 40.7; H, 5.1; N, 5.3%; Relevant IR bands: ν = 3450 (br), 2970 (w), 2920 (w), 2850 (w), 1608 (s), 1455 (s), 1400 (s), 1123 (s), 1048 (w), 1017 (w), 908 (w), 771 (w), 665 (w), 560 (w) cm−1. The same reaction was performed with the racemic mixture of Hmpm ligand with the aim to perform the crystallographic characterization of the crystals (discussed in further sections).

[Ni4(R-mpm)4(t-butCOO)4]·H2O (2R) and [Ni4(S-mpm)4 (t-butCOO)4] (2S). The R- or the S-enantiomer of Hmpm (0.6 mmol, 0.074 g) was dissolved in MeCN (20 mL). To this solution were added NEt3 (1.2 mmol, 0.167 mL), pivalic acid (t-butCOOH; 0.6 mmol, 0.069 mL), and Ni(ClO4)2·6H2O (0.6 mmol, 0.22 g), respectively. The reaction mixture was then stirred at room temperature for 20 min. Green crystalline blocks of 2R and 2S were obtained via the slow evaporation of the reaction mixture at 0 °C after 1 day. The yields were 39% and 40% for 2R and 2S, respectively. Anal. calcd for C44H70N4Ni4O13 (2R·H2O): C, 50.31; H, 6.16; N, 4.89%. Found: C, 50.45; H, 6.00; N, 4.92%. Relevant IR bands: ν = 2953 (mb), 1606 (m), 1560 (s), 1530 (s), 1481 (s), 1427 (s), 1358 (m), 1283 (m), 1223 (m), 1107 (m), 1082 (m), 900 (m), 771 (mb), 662 (m), 564 (m), 478 (m), 426 (m) cm−1.

RESULTS AND DISCUSSION

Structural description

As expected, all three complexes crystallize in chiral space groups. The structures of 1 and 2 have a common core that consists of a Ni4O4 cubane-like unit that has a two-fold rotation axis that passes through the centre of the cube, the vertices of which are occupied by four NiII cations and four μ3-Oatoms (Ni1, Ni2, O1 and O2 and symmetry related). A labelled plot is shown in Fig. 1 and selected bond lengths and angles are summarized in Table 1. Each crystallographically unique NiII ion has a distorted octahedral geometry. The coordination sites of the NiII cations are fulfilled by four carboxylates and four mpm− ligands that provide the four μ3-O donors (η1:η3:μ3), resulting in neutral charged clusters. Two carboxylates act as a bridge between Ni1 and Ni2 in its syn–syn coordination mode (η1:η1:μ) and the other two carboxylates act as bidentate chelating ligands (Scheme 1). The N2O4 coordination environment of Ni1 is fulfilled by two mpm− ligands, one μ3-O donor from another mpm− ligand and one O atom from one syn–syn carboxylate, whereas the O6 environment of Ni2 comes from three μ3-O ligands, one bidentate chelating carboxylate and one O atom from a syn–syn carboxylate. The Ni4O4 cubane core is very distorted. The two faces that bind the syn–syn carboxylates are not planar i.e. the dihedral angle between Ni1–O1–O2 and Ni2–O1–O2 is close to 28°, with Ni–O–Ni bond angles less than 90°, whereas the other four faces are roughly planar with bond angles close to 100°. Although the cubanes are similar in their general trends, there are many differences in their crystal packing (Fig. 2). Complexes 1 show layers of cubanes alternatively reversed by 180° and forming a large set of H-bonds involving the O-carboxylate atoms and the solvent molecules in the crystal lattice. In contrast, the hydrophobic shells of complexes 2 isolate efficiently the clusters, allowing less space to host polar solvent molecules and thus reducing the H-bonding interactions. The shortest distance between the centroids of neighbouring cubanes is 10.339 Å for the acetato complexes and 12.053 Å for the pivalato clusters, consistent with the larger size of the tert-butyl substituents in the latter.

Discussion pertaining to cubane-like clusters

The small N···M···O bite angles (M = metal) induced by the 2-pyridinemethanol ligand and its substituted derivatives (L in the following formulas of this section), combined with the μ3 ability of the O-donor, are adequate features to build cubanelike clusters that typically have the general formula [M4(L)4(X)4(S)x], where X− is a monoanionic ligand and S are solvent molecules.7–13 Very frequently, x = 4 for monodentate X− ligands (i.e., Cl−, N3−, carboxylates), zero for bidentate ligands (typically carboxylates), or x = 2 for intermediate cases. Coordination of four bidentate L ligands to the {M4O4} core is not trivial and can be achieved in three main arrangements: one ligand linked to each cation arranged in two pairs of parallel ligands rotated by 90° between them (Fig. 3-A); one ligand linked to each cation with the four ligands parallel between them (Fig. 3-B); or two pairs of ligands linked to only two cations (Fig. 3-C). The A arrangement is by far the most common for M = FeII,7

CoII,8 NiII,9 CuII and ZnII;10,11 the Barrangement has been reported in few cases for {Ni4O4} cubanes,9f,j,p,12a and once for {Co4O4}12b and {Cu4O4}12c cubanes, whereas the C-coordination has never been reported for homometallic {M4O4} cubanes. However, the C-arrangement is the preferred for heterometallic {M2M′2O4} or {M3M′O4} cubanes (M = CoII or NiII, M′ = MnIII or LnIII) in which M′ is more oxophilic than the CoII or NiII cations.13

The ideal cubane structure is highly symmetrical (Td) but the presence of four bidentate ligands reduces drastically the symmetry of the clusters, being S4 for the A-arrangement, D2 for the B-arrangement and C2 for the C type. The A-type cubanes are intrinsically achiral due to the presence of the S4 improper rotation axis but interestingly, the dissymmetric D2 and C2 groups are intrinsically chiral, Fig. 3. The preparation of chiral systems from achiral components is unusual, and as can be expected, the achiral type-A cubanes are the predominant arrangement.

The analysis of the structural data for the B-type cubanes reveals that they are closely related to the presence of substituted pym− ligands that are chiral or bearing large substituents.9f,k,p,12 The cubanes belonging to the C-type show a lower symmetry, containing two different cations and an heterometallic core profiting from its different oxophilic character. In all of the reported cases, B and C-type cubanes show both enantiomers related by an inversion centre in the network, but the subsequent resolution to obtain enantiomerically pure chiral cubes was unsuccessful.

Complexes 1 and 2 exhibit a C-type core that has never been previously reported for homometallic cubanes. The reason for this observation is directly related to the employment of the chiral mpm− ligand and the transfer of this chirality as the driving force.

For the A-type cubanes with only one bidentate ligand coordinated to each NiII cation, transfer of chirality resulting in octahedral chiral centres is not possible and the S4 symmetry excludes this possibility due to the chiral character of the ligands. In the same way, the B-type could be possible, thus yielding chiral cubanes in which the transfer of chirality is only possible to the cluster, but not to the cations, because of the same reason as in the A-type. In contrast, the C-type core promotes the transfer of chirality to the Ni1/Ni1′ cations, which are coordinated to four bidentate ligands with the ΔΔ configuration for the enantiomer containing the (R)-mpm−ligands and the ΛΛ configuration for the enantiomer containing the (S)-mpm− ligands. In addition, the asymmetric arrangement of the mpm− and carboxylate ligands around the {Ni4O4} core determines the chirality of the entire cubane systems, Fig. 4, resulting in the maximum transfer of chirality from the ligand to the molecule.

The reaction of the racemic mixture of Hmpm with nickel acetate is noteworthy to reinforce these conclusions. The simultaneous presence of both enantiomers of the ligand could a priori allow several arrangements: the cubane with A-shape containing (R) and (S)-mpm− and S4 symmetry, the two enantiomeric cubanes in the same network related by inversion centers/planes or the separate crystallization of enantiomerically pure crystals of each enantiomer. The experimental result of this reaction allowed the characterization of enantiomeri cally pure crystals of complexes 1, supporting the maximum transference of chirality.

Electronic circular dichroism (ECD) studies

Electronic circular dichroism confirms the enantiomeric nature of the 1R/1S and 2R/2S pairs of complexes. The spectra are characterized by three absorptions. As a representative example, the spectrum of 1S collected in methanol solution exhibits positive Cotton effects at λmax = 230, 270 and 310 nm and a weak negative Cotton effect at 385 nm, whereas 1R is the mirror image with absorptions at the same wavelengths but with the opposite sign, Fig. 5. The spectra of 2R/2S recorded in dichloromethane show the same signals at λmax = 280 and 330 nm (positive) and the weak signal at 397 nm (negative).

The spectra recorded in the solid state for 1R/1S show the same absorptions with the same signs shifted ~10–20 nm to higher wavelengths with respect to the methanolic solution (243, 280, 328 and 423 nm). The agreement between the solid and solution spectra indicates that the clusters are stable in solution, independently of the polarity of the solvent.

Magnetic properties

The magnetic response is not dependent on its R or S chirality and thus, the measurements were performed for one of the enantiomers of each compound. The susceptibility measurements for 1R and 2R reveal a very similar response between them as can be expected from the similar structural information (Fig. 6). Room temperature χMT values for 1R/2R are 5.07/4.85 cm3 mol−1 K, larger than the theoretical value of 4.00 cm3 mol−1 K (g = 2.0) for four isolated S = 1 spins. On cooling, the χMT values are quasi constant between 300 and 100 K and below 50 K they show a fast decrease and tend to zero at low temperature. The presence of clear χM maxima at 12.5/17 K indicates an overall antiferromagnetic response and an S = 0 ground state and weak magnetization under the maximum applied field of 5 T, Fig. 6, inset, due to the partial population of the closer excited spin states, ESI Fig. S1.†

A fit of the experimental data was performed on the basis of the structural data that show three opposite pairs of faces with different bond parameters among them, Scheme 2.

For an antiferromagnetic system that tends to zero susceptibility at low temperature, it is not necessary to consider the anisotropy of the cations and therefore the experimental data were fitted with the PHI program14 applying the isotropic Hamiltonian:

$$H = -2J_1(S_1 \cdot S_2 + S_3 \cdot S_4) - 2J_2(S_1 \cdot S_4 + S_2 \cdot S_3) - 2J_3(S_1 \cdot S_3 + S_2 \cdot S_4)$$

Preliminary fits with this three-J Hamiltonian show similar values for J2 and J3 and thus the fit was simplified assuming J2 = J3. The best fit parameters are J1 = 3.1 cm−1, J2 = J3 = −2.5 cm−1, g = 2.28 and R = 1.4 × 10−4 for 1R and J1 = 6.0 cm−1, J2 = J3 = −3.1 cm−1, g = 2.22 and R = 6.1 × 10−5 for 2R. As an example, a fit of the magnetization data for 1R was satisfactory, affording the very similar

exchange parameters J1 = 3.1 cm−1, J2 = J3 = −2.5 cm−1, g = 2.28, Fig. 6 inset. For the {Ni4(μ3-OR)4} cubane topology it has been well established that there is a magneto-structural correlation between the value of the Ni–O–Ni bond angles of each face and the sign and magnitude of the superexchange interaction. The ferro-antiferromagnetic (FM/AF) border has been calculated to be around 99°, allowing ferromagnetic interactions for smaller bond angles and antiferromagnetic coupling for larger angles.15 For strongly distorted cubanes, such as 1 and 2, it is not simple to justify the S = 0 ground state and the sign of the interactions as solely being due to the presence of different distortions in the Ni–O–Ni bond angles, the Ni–O–Ni–O torsion angles and the presence of additional carboxylate bridges. To understand the coupling in the above described compounds, we have reviewed the metrical parameters and the magnetic response of the {Ni4(pym)4} cubanes for which the magnetic susceptibility data are available in the literature.

Firstly, we realized that all studied [Ni4(pym)4(X)4(S)4] cubanes, where X− is a monoanionic ligand and S are solvent molecules, belonging to the A-type system, give a ferromagnetic response with a well-defined S = 4 ground state. It is noteworthy that even with low barriers for the reversal of the magnetization, some of these complexes exhibit single-molecule magnetic (SMM) behavior.9c,d Structurally, these cubanes are quite regular, with Ni–O–Ni bond angles close to the FM/ AF border, being slightly larger for the two opposite top faces that coordinate the pym− ligands, than the other four side faces, Table 2. The six faces of the cubanes are roughly planar with very small or negligible Ni–O–Ni–O torsion angles, Fig. 7.

In contrast, the systems containing syn–syn carboxylate bridges with the formula [Ni4(pym)4(μ-RCOO)2(X)2(S)2] or [Ni4(pym)4(μ-RCOO)4] exhibit an overall antiferromagnetic response and an S = 0 ground state. These systems belong to the A- or B-types and are characterized by strong distortions in their cubane cores. The most important distortion is derived from the bite angle of the carboxylate ligand that requires slightly shorter Ni⋯Ni distances to achieve the coordination, thus reducing the Ni–O–Ni bond angles to 90°, or lower, and inducing an appreciable Ni–O–Ni–O torsion angle, Fig. 7 and Table 2. For the systems with four faces linking syn–syn carboxylates, the two top faces coordinating the pym− ligands increase the Ni–O–Ni bond angles up to 103°. In some cases, it has been postulated that the antiferromagnetic contribution of the carboxylate bridge can promote AF coupling independently of the reduction in the Ni–O–Ni bond angles.12a,16 However, studies on FM dinuclear {Ni2(μ-OR)2(μ-RCOO)} systems17 with similar bond parameters or cubanes with [Ni4(μ3-OR)4(μ-RCOO)2] cores and S = 4 ground states demonstrate that there is always some ferromagnetic character in this pathway.18 In light of these data it seems reasonable to assign the ferromagnetic interaction parametrized by J1 to the Ni1⋯Ni2 interactions and the antiferromagnetic interactions to the other four superexchange pathways within the cubane cores of 1 and 2.

CONCLUSIONS

In conclusion, two pairs of enantiomeric cubane-like {Ni4(pym)4} clusters have been characterized. The reported systems are the first NiII complexes derived from the ligand 2-(1-hydroxyethyl)pyridine (Hmpm). The chiral character of the ligand promotes the transfer of chirality to the NiII cations and the cubane core resulting in an unprecedented homometallic asymmetric motif. The topology of the {Ni4(R-pym)4} cubanes has been reviewed and their magnetic response, that can be FM (ground spin state S = 4) or AF (ground spin state S = 0), has been correlated to the [Ni4(pym)4(X)4(S)4] formula and the distortions derived from the coordination of the X = carboxylate ligands. Comparisons of racemic or achiral clusters versus their chiral counterparts is a poorly explored field that offers interesting perspectives derived from their potential structural differences and their derived properties.

ACKNOWLEDGEMENTS

A. E and J. M thank the financial support from Ministerio de Economía y Competitividad-Spain, Project PGC2018-094031- B-100. This work was also supported by NSERC-DG (Th. C. S, M. P), ERA (Th. C. S), CFI (M. P) and Brock University (Chancellor's Chair for Research Excellence; Th. C. S).

NOTES AND REFERENCES

1 (a) D. Carmona, P. Lamata, A. Sanchez, P. Pardo, R. Rodriguez, P. Ramirez, F. J. Lahoz, P. Garcia-Orduna and L. A. Oro, Dalton Trans., 2014, 43, 15546; (b) D. Carmona, P. Lamata, A. Sanchez, P. Pardo, R. Rodriguez, P. Ramirez, F. J. Lahoz, P. Garcia-Orduna and L. A. Oro, Organometallics, 2014, 33, 4016; (c) P. Horeglad, M. Cybularczyk, A. Litwinska, A. M. Dabrowska, M. Dranka, G. Z. Zukowska, M. Urbanczyk and M. Michalak, Polym. Chem., 2016, 7, 2022.

2 S. Chorazy, M. Reczynski, R. Podgajny, W. Nogas, S. Buda, M. Rams, W. Nitek, B. Nowicka, J. Mlynarski, S.-I. Ohkoshi and B. Sieklucka, Cryst. Growth Des., 2015, 15, 3573.

3 (a) S. Chorazy, R. Podgajny, W. Nogas, S. Buda, W. Nitek, J. Mlynarski, M. Rams, M. Koziel, E. J. Galazka, V. Vieru, L. F. Chibotaru and B. Sieklucka, Inorg. Chem., 2015, 54, 5784; (b) S. Chorazy, R. Podgajny, W. Nitek, T. Fic, E. Gorlich, M. Rams and B. Sieklucka, Chem. Commun., 2013, 49, 6731; (c) P. Konieczny, L. Michalski, R. Podgajny, S. Chorazy, R. Pelka, D. Czernia, S. Buda, J. Mlynarski, B. Sieklucka and T. Wasiutynski, Inorg. Chem., 2017, 56, 2777; (d) Z.-G. Gu, X.-H. Zhou, Y.-B. Jin, R.-G. Xiong, J.-L. Zuo and X.-Z. You, Inorg. Chem., 2007, 46, 5462; (e) P. Abbasi, K. Quinn, D. I. Alexandropoulos, M. Damjanovic, W. Wernsdorfer, A. Escuer, J. Mayans, M. Pilkington and T. C. Stamatatos, J. Am. Chem. Soc., 2017, 139, 15644.

4 (a) M. Liu, L. Zhang and T. Wang, Chem. Rev., 2015, 115, 7304; (b) R. Carr, N. H. Evans and D. Parker, Chem. Soc. Rev., 2012, 41, 7673.

5 (a) J. Crassous, Chem. Soc. Rev., 2009, 38, 830; (b) P. Xing And Y. Zhao, Acc. Chem. Res., 2018, 51, 2324.

6 G. M. Sheldrick, SHELXL-2014/7: Program for the Solution of Crystal Structures, University of Göttingen, Göttingen, Germany, 2014.

7 F. Piga, F. Moro, I. Krivokapic, A. J. Blake, R. Edge, E. J. L. McInnes, D. J. Evans, J. McMaster and J. Van Slageren, Chem. Commun., 2012, 48, 2430.

8 (a) E.-C. Yang, D. N. Hendrickson, W. Wernsdorfer, L. N. Zakharov, R. D. Sommer and A. L. Rheingold, J. Appl. Phys., 2002, 91, 7382; (b) S. G. Telfer, R. Kuroda, J. Lefebvre and D. B. Leznoff, Inorg. Chem., 2006, 45, 4592; (c) F.-M. Wang, C.-S. Lu, Y.-Z. Li and Q.-J. Meng, Acta Crystallogr., Sect. E: Struct. Rep. Online, 2010, 66, m594.

9 (a) K. Bizilj, S. G. Hardin, B. F. Hoskins, P. J. Oliver, E. R. T. Tiekink and G. Winter, Aust. J. Chem., 1986, 39, 1035; (b) A. Escuer, M. Font-Bardia, S. B. Kumar, X. Solans and R. Vicente, Polyhedron, 1999, 18, 909; (c) E.-C. Yang, W. Wernsdorfer, S. Hill, R. S. Edwards, M. Nakano, S. Maccagnano, L. N. Zakharov, A. L. Rheingold, G. Christou and D. N. Hendrickson, Polyhedron, 2003, 22, 1727; (d) E.-C. Yang, W. Wernsdorfer, L. N. Zakharov, Y. Karaki, A. Yamaguchi, R. M. Isidro, G.-D. Lu, S. A. Wilson, A. L. Rheingold, H. Ishimoto and D. N. Hendrickson, Inorg. Chem., 2006, 45, 529; (e) J. Lawrence, E.-C. Yang, R. Edwards, M. M. Olmstead, C. Ramsey, N. S. Dalal, P. K. Gantzel, S. Hill and D. N. Hendrickson, Inorg. Chem., 2008, 47, 1965; (f) S. G. Telfer, N. D. Parker, R. Kuroda, T. Harada, J. Lefebvre and D. B. Leznoff, Inorg. Chem., 2008, 47, 209; (g) F.-M. Wang, J.-G. Lin, Y.-Y. Xing, Y.-M. Liu, C.-S. Lu and Q.-J. Meng, J. Coord. Chem., 2010, 63, 3431; (h) J. Zhang, P. Teo, R. Pattacini, A. Kermagoret, R. Welter, G. Rogez, T. S. A. Hor and P. Braunstein, Angew. Chem., Int. Ed., 2010, 49, 4443; (i) F. Moro, F. Piga, I. Krivokapic, A. Burgess, W. Lewis, J. McMaster and J. Van Slageren, Inorg. Chim. Acta, 2010, 363, 4329; (j) J.-P. Sun, L.-C. Li and X.-J. Zheng, Inorg. Chem. Commun., 2011, 14, 877; (k) W.-H. Zhang, N. B. Sulaiman, P. X. S. Tio and T. S. A. Hor, CrystEngComm, 2011, 13, 2915; (l) K. I. Alexopoulou, C. P. Raptopoulou, V. Psycharis, A. Terzis, V. Tangoulis, T. C. Stamatatos and S. P. Perlepes, Aust. J. Chem., 2012, 65, 1608; (m) A. Scheurer, J. Korzekwa, T. Nakajima, F. Hampel, A. Buling, C. Derks, M. Neumann, L. Joly, K. Petukhov, K. Gieb, P. Muller, K. Kuepper and K. Meyer, Eur. J. Inorg. Chem., 2015, 1872; (n) H. Golchoubian and S. Kazemi, J. Coord. Chem., 2016, 69, 447; (o) J. Korzekwa, A. Scheurer, F. W. Heinemann, W. Kroener, K. Gieb, P. Muller and K. Meyer, J. Coord. Chem., 2017, 70, 626; (p) Y.-Q. Yuan, F.-L. Yuan, F.-L. Li, Z.-M. Hao, J. Guo, D. J. Young, W.-H. Zhang and J.-P. Lang, Dalton Trans., 2017, 46, 7154; (q) Z.-M. Hao, M.-Y. Chao, Y. Liu, Y.-L. Song, J.-Y. Yang, L. Ding, W.-H. Zhang and J.-P. Lang, Dalton Trans., 2018, 47, 8865.

10 (a) J. Moncol, K. Jomova, L. Zelenicky, T. Lis and M. Valko, Acta Crystallogr., Sect. C: Cryst. Struct. Commun., 2011, 67, m318; (b) H.-M. Lv, S.-N. Wang, D.-C. Li and J.-M. Dou, Acta Crystallogr., Sect. C: Cryst. Struct. Chem., 2014, 70, 843; (c) X. Zhang, B. Li and J. Zhang, Inorg. Chem., 2016, 55, 3378; (d) A. Escuer, J. Mayans and M. Font-Bardia, Dalton Trans., 2016, 45, 1604.

11 (a) E.-C. Yang, C. Kirman, J. Lawrence, L. N. Zakharov, A. L. Rheingold, S. Hill and D. N. Hendrickson, Inorg. Chem., 2005, 44, 3827; (b) J. Lawrence, C. C. Beedle, E.-C. Yang, J. Ma, S. Hill and D. N. Hendrickson, Polyhedron, 2007, 26, 2299; (c) C. C. Beedle, J. J. Henderson, P.-C. Ho, T. Sayles, M. Nakano, J. R. O'Brien, K. J. Heroux, E. del Barco, M. B. Maple and D. N. Hendrickson, Inorg. Chem., 2010, 49, 5780.

12 (a) C. G. Efthymiou, C. Papatriantafyllopoulou, N. I. Alexopoulou, C. P. Raptopoulou, R. Boca, J. Mrozinski, E. Bakalbassis and S. P. Perlepes, Polyhedron, 2009, 28, 3373; (b) F. Evangelisti, R. Guttinger, R. More, S. Luber and G. R. Patzke, J. Am. Chem. Soc., 2013, 135, 18734; (c) L. Alvarez-Miguel, H. Barbero, A. Sacristan-Martin, J. M. M. Alvarez, A. Perez-Encabo, C. M. Alvarez, R. Garcia-Rodriguez and D. Miguel, Inorg. Chem., 2017, 57, 264.

13 (a) X.-Q. Zhao, Y. Lan, B. Zhao, P. Cheng, C. E. Anson and A. K. Powell, Dalton Trans., 2010, 39, 4911; (b) Y.-Z. Yu, Y.-H. Shen, L. Lv, P. Gao, C.-P. Zhao and D.-C. Li, Chin. J. Struct. Chem., 2011, 30, 1393; (c) P. Wang, S. Shannigrahi, N. L. Yakovlev and T. S. A. Hor, Inorg. Chem., 2012, 51, 12059; (d) P. Wang, S. Shannigrahi, N. L. Yakovlev and T. S. A. Hor, Chem. – Asian J., 2013, 8, 2943; (e) W.-R. Yu, G.-H. Lee and E.-C. Yang, Dalton Trans., 2013, 42, 3941; (f) P. Wang, S. Shannigrahi, N. L. Yakovlev and T. S. A. Hor, Dalton Trans., 2014, 43, 182.

14 N. F. Chilton, R. P. Anderson, L. D. Turner, A. Soncini and K. S. Murray, J. Comput. Chem., 2013, 34, 1164. 15 (a) M. A. Halcrow, J.-S. Sun, J. C. Huffman and G. Christou, Inorg. Chem., 1995, 34, 4167; (b) K. Isele, F. Gigon, A. F. Williams, G. Bernardinelli, P. Franz and S. Decurtins, Dalton Trans., 2007, 332.

16 G. Aromi, A. S. Batsanov, P. Christian, M. Helliwell, O. Roubeau, G. A. Timco and R. E. P. Winpenny, Dalton Trans., 2003, 4466.

17 K. K. Nanda, R. Das, L. K. Thompson, K. Venkatsubramanian and K. Nag, Inorg. Chem., 1994, 33, 5934.

18 (a) G. Chaboussant, R. Basler, H. U. Gudel, S. T. Ochsenbein, A. Parkin, S. Parsons, G. Rajaraman, A. Sieber, A. A. Smith, G. A. Timco and R. E. P. WinpennyX, Dalton Trans., 2004, 2758; (b) R. M. Elmehdawi, M. N. EL-Kaheli, R. G. Abuhmaiera, F. A. Treish, M. M. B. Younes, C. Bazzicalupi, A. Guerri, A. Caneschi and A. Amjad, Materials, 2017, 10, 178; (c) A. K. Ghosh, M. Shatruk, V. Bertolasi, K. Pramanik and D. Ray, Inorg. Chem., 2013, 52, 13894.

Legends to figures

Scheme 1. (top) A plot of the Hmpm ligand (asterisk denotes the chiral C-atom); (bottom) Coordination modes for mpm− and carboxylate ligands found in the complexes reported in this work.**Figure. 1** (top) Mirror image of 1R and 1S; (bottom) the labelled common core for 1R, 1S and 2R.

Figure.2 Packing of complexes 1 (top) and 2 (bottom) showing the different arrangement due to the size and polarity of the methyl- and tert-butyl substituents of the carboxylate function.

Figure.3 (top) View of the three arrangements of four bidentate ligands around the {M4O4} core; (bottom) symmetry elements for the three cases.

Figure.4. (top) View of the Δ or Λ configuration around the Ni1 cations for 1R/2R and 1S/2S, respectively; (bottom) view of the R and S cubanes along the C2 axis showing the chirality of the molecules. Bidentate carboxylates and one of the mpm− ligands have been emphasized for clarity.

Figure.5 ECD spectra for complexes 1R/1S in the solid state (top) or methanolic solution (middle) and 2R/2S (bottom). Red and black lines correspond to (R) and (S) enantiomers, respectively.

Figure.6 χMT vs. temperature plots for complexes 1R (red) and 2R (blue). Insets; χM vs. T plots showing the susceptibility maxima and magnetization vs. field for 1R showing the low magnetization due to close $S \neq 0$ lying spin levels.

Scheme 2 Left, coupling scheme for complexes 1 and 2. J1 refers to the faces that coordinate the syn–syn carboxylates. Right, spin arrangement from the calculated J values that justify the $S = 0$ ground state.

Figure.7 {NiII4} cubane cores derived from the pym− ligand without (left) or with two (middle) and four (right) carboxylate coligands. The two top faces that coordinate the pym− ligands are highlighted in orange.

443 **SCHEME 1**

444

445

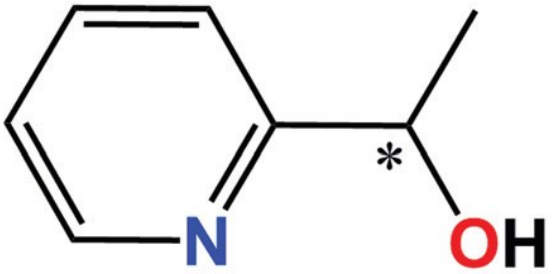

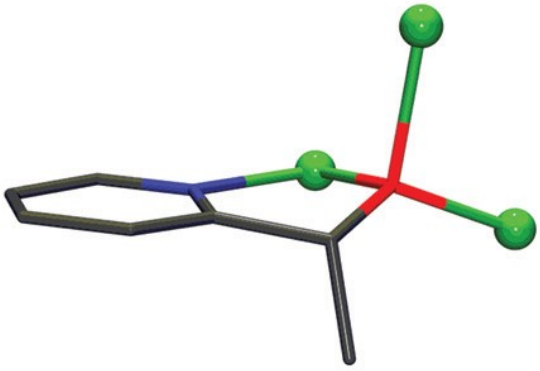

$\eta^1:\eta^3:\mu_3$

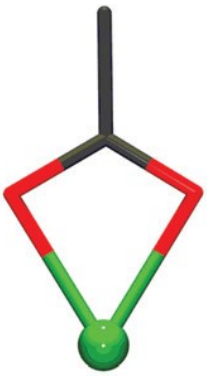

bidentate chelating

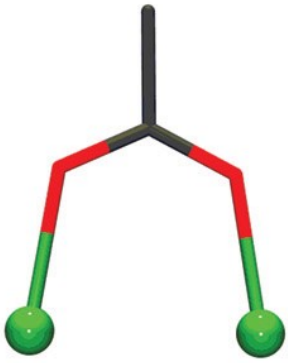

$\eta^1:\eta^1:\mu$

446

447

448 **FIGURE 1**

449

450

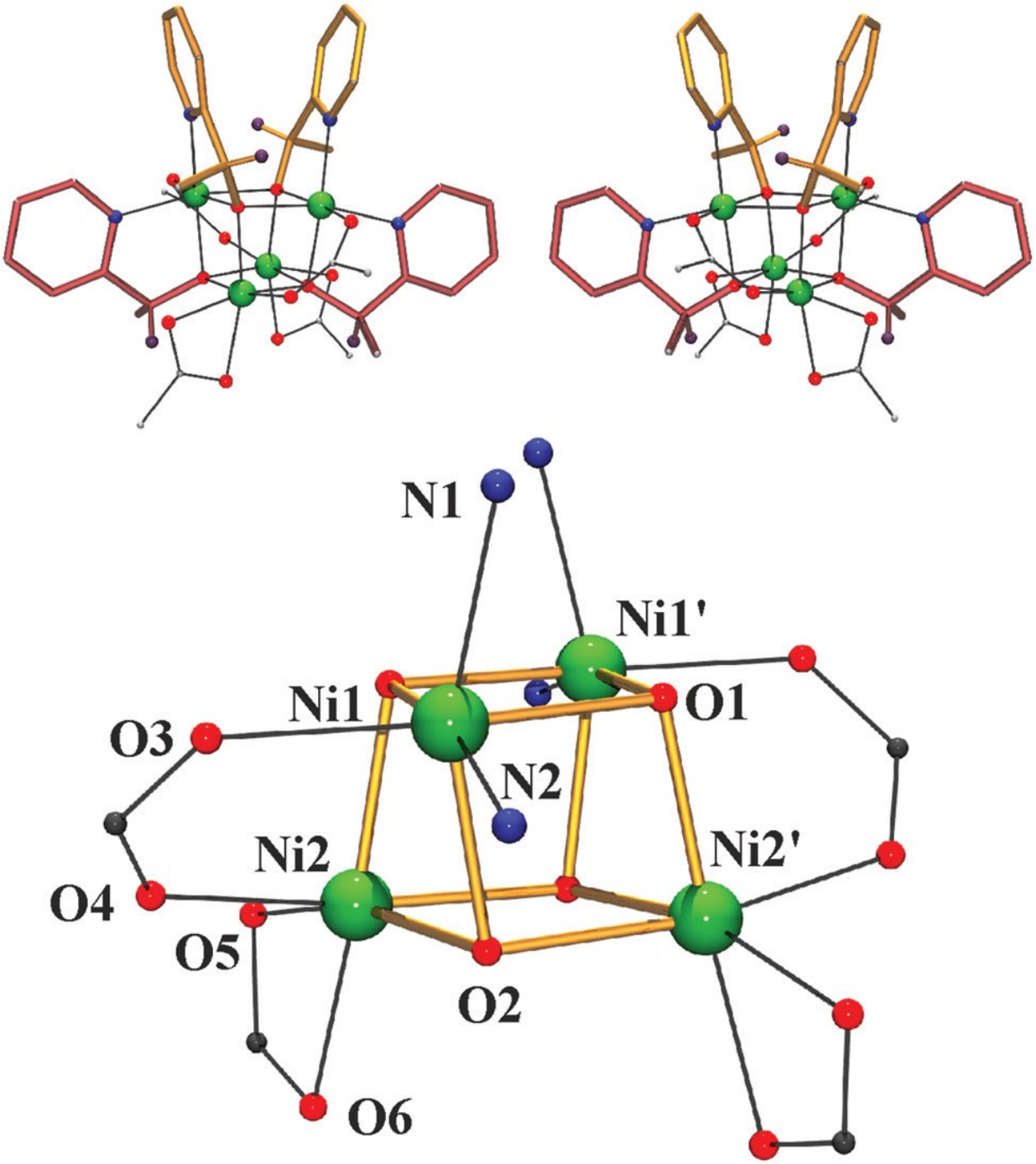

451

452

453

454 **FIGURE 2**

455

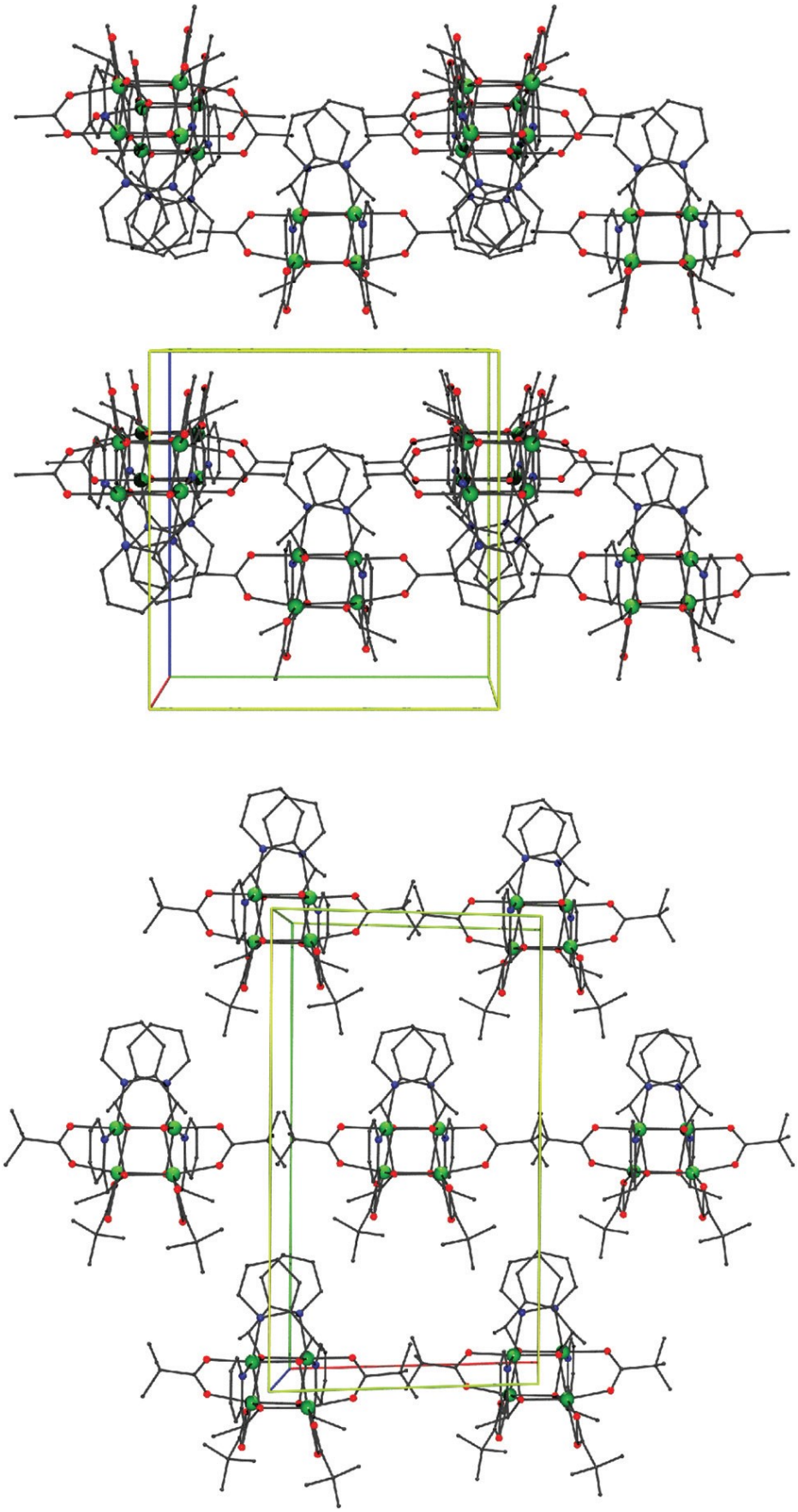

456

457 **FIGURE 3**

458

459

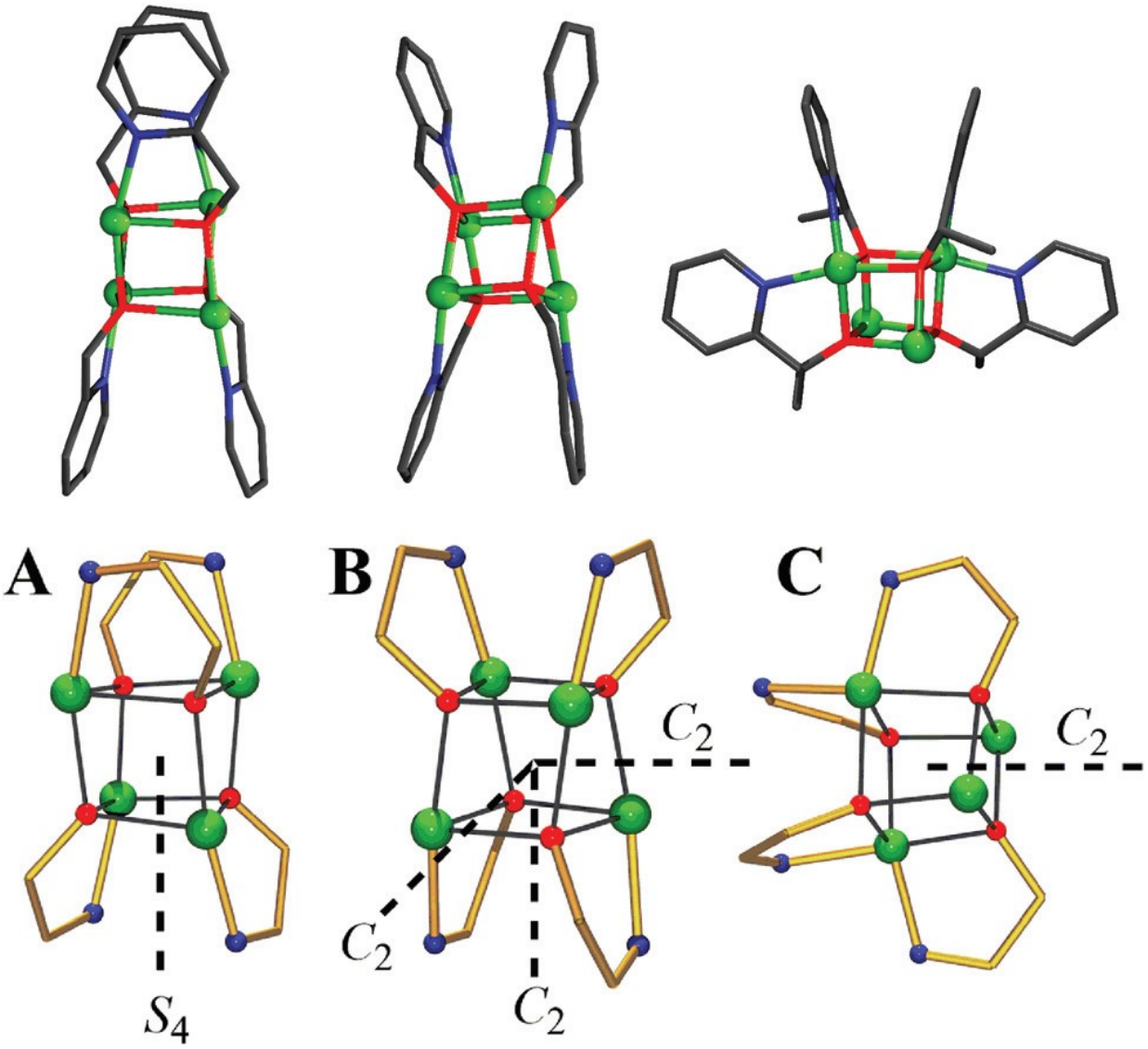

460

461

462 **FIGURE 4**

463

464

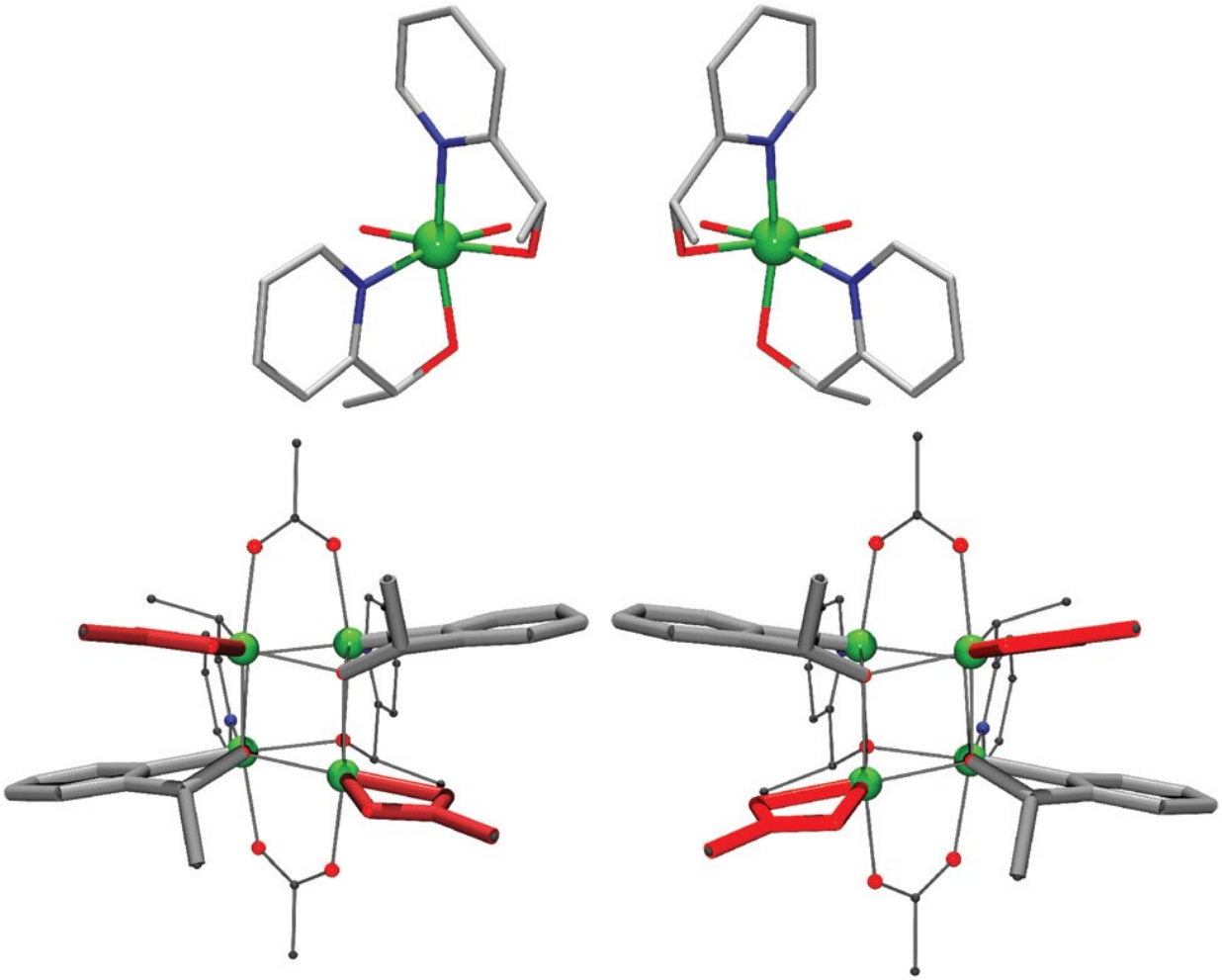

465

466

467 **FIGURE 5**

468

469

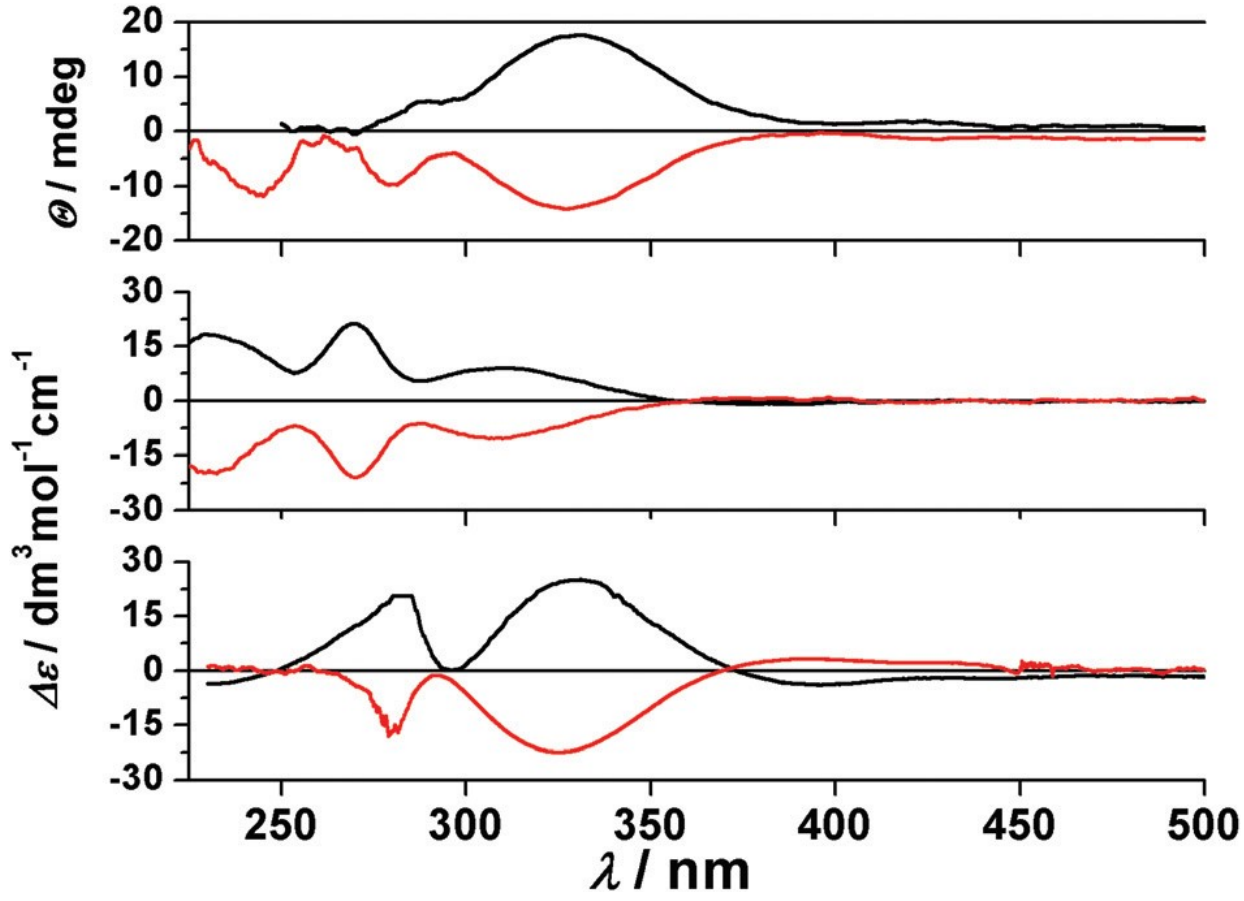

470

471

472 **FIGURE 6**

473

474

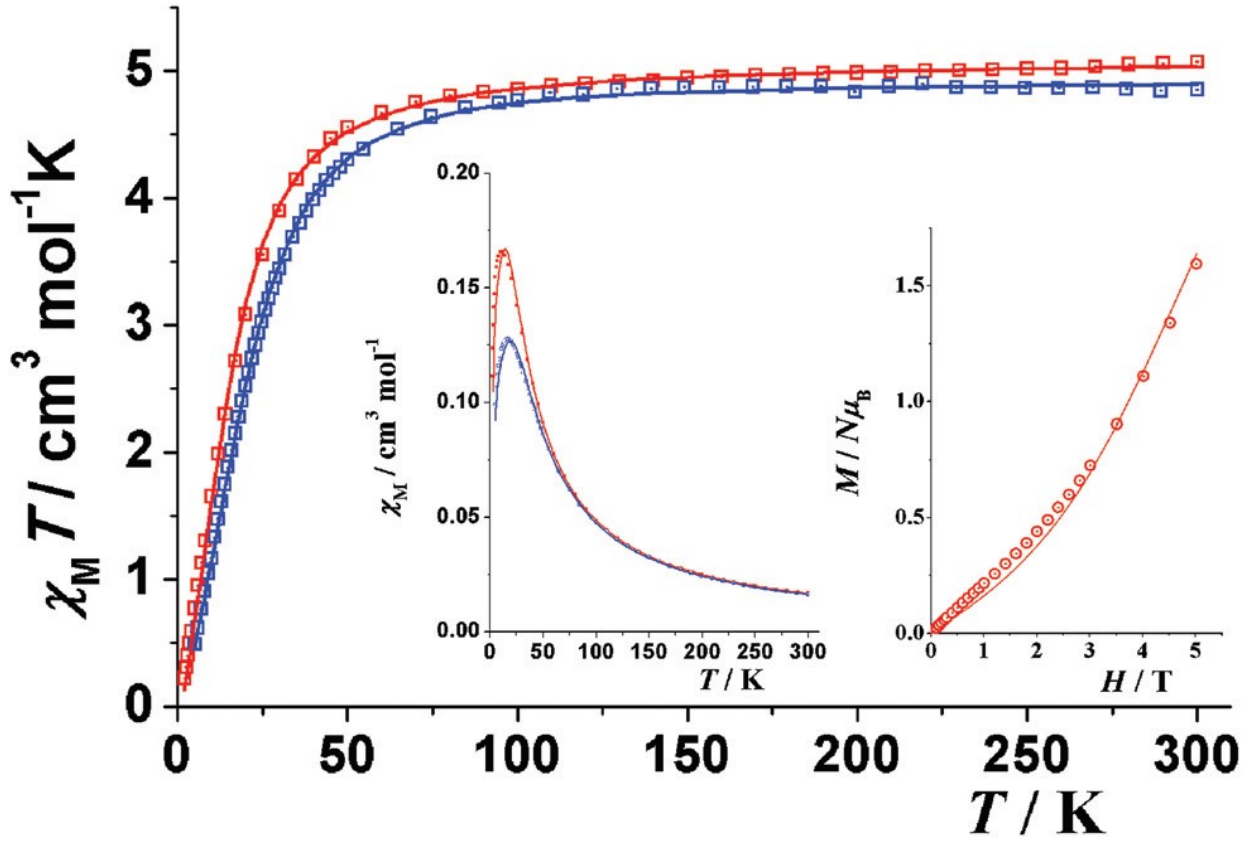

475

476

477 **SCHEME 2**

478

479

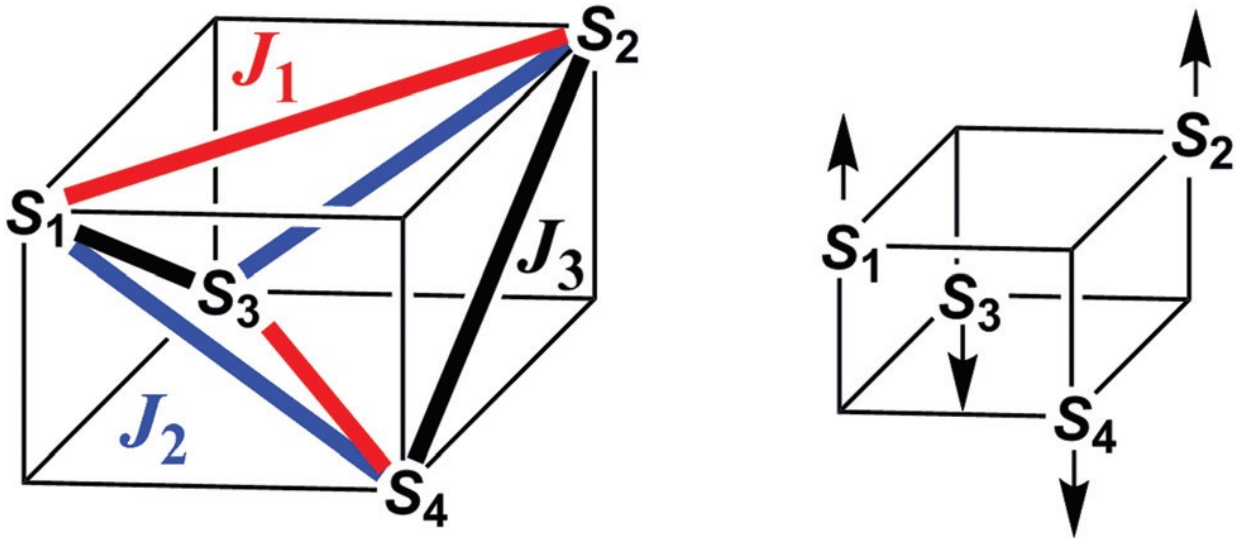

480

481

FIGURE 7

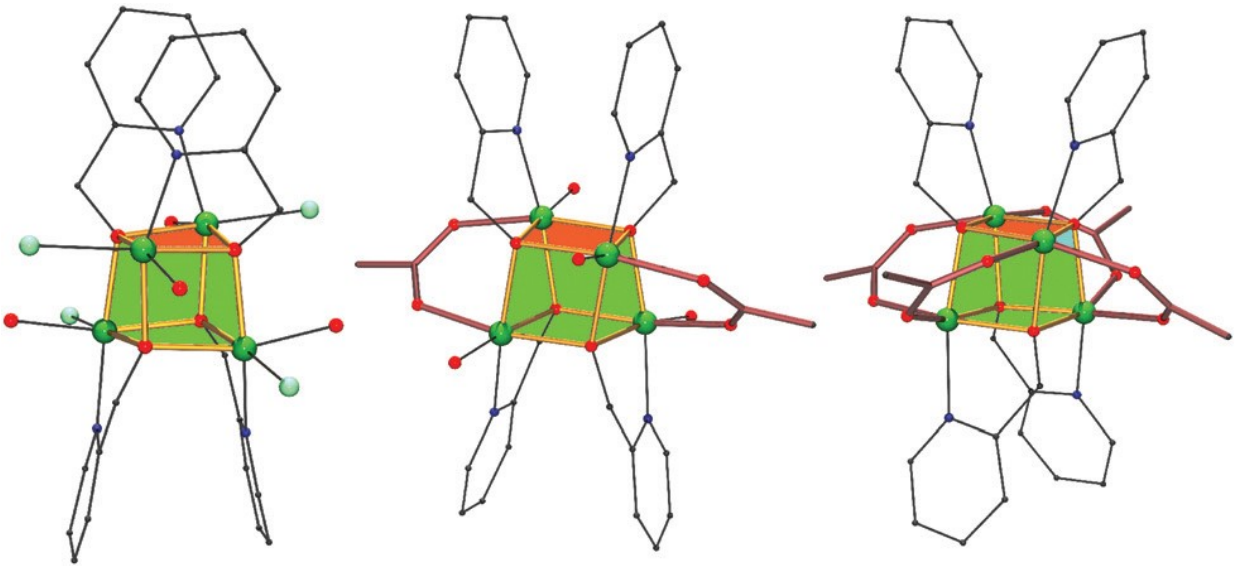

Table 1 Main bond distances (Å) and angles (°) for complexes 1R, 1S and 2R

	1*R*	1*S*	2*R*
Ni(1)–O(1)	2.039(4)	2.039(3)	2.057(7)
Ni(1)–O(2)	2.057(5)	2.054(3)	2.060(8)
Ni(1)–O(1′)	2.095(5)	2.071(3)	2.106(5)
Ni(1)–O(3)	2.060(5)	2.047(3)	2.062(6)
Ni(1)–N(1)	2.065(6)	2.058(3)	2.048(6)
Ni(1)–N(2)	2.067(6)	2.075(4)	2.071(6)
Ni(2)–O(1′)	2.039(5)	2.048(3)	2.062(5)
Ni(2)–O(2)	2.051(5)	2.107(3)	2.084(5)
Ni(2)–O(2′)	2.089(5)	2.081(3)	2.106(5)
Ni(2)–O(4)	2.030(5)	2.031(3)	2.032(7)
Ni(2)–O(5)	2.101(5)	2.111(4)	2.152(6)
Ni(2)–O(6)	2.082(5)	2.110(4)	2.104(6)
Ni(1)–O(1′)–Ni(2)	88.3(2)	88.7(1)	88.1(3)
Ni(1)–O(2)–Ni(2)	89.0(2)	97.2(1)	88.8(3)
Ni(1)–O(1)–Ni(1′)	100.3(2)	101.0(1)	100.5(2)
Ni(1)–O(1)–Ni(2′)	99.5(2)	99.6(1)	100.2(3)
Ni(2)–O(2)–Ni(2′)	102.7(2)	101.5(1)	101.7(2)
Ni(1)–O(2)–Ni(2′)	97.3(2)	88.3(1)	98.7(3)

490 **Table 2** Bond parameters and magnetic response (FM or AF response, S ground state) for the reported
491 cubanes derived from 2-pyridinemethanol

492

Compound[a]	Ni–O–Ni (Top faces)	Ni–O–Ni (Other faces)	Ni–O–Ni–O (Top faces)	Ni–O–Ni–O (Other faces)	Type	FM/AF; S	Ref.
$[Ni_4(pym)_4X_4S_4]$							
AKISUI	99.6	98.6; 96.6	6.4	9.8	A	FM; $S = 4$	9d
AKISOC[b]	99.2	97.1; 98.6	7.2	9.7–9.5	A	FM; $S = 4$	9d
	100.5	98.4; 96.5	5.3	10.7			
BEPBED[b]	101.4	98.6; 97.1	5.5	11.6	A	FM; $S = 4$	9d
	99.7	99.2; 97.4	7.5	10.2			
HECNIN[b]	100.1; 99.8	97.8; 96.2	4.9	10.1	A	FM; $S = 4$	9d
	99.5; 99.3	99.2; 96.3	6.4	9.7			
HECNOT	99.2	98.9; 96.9	7.3	9.4	A	FM; $S = 4$	9d
HECNUZ	99.5	98.6; 96.5	6.4	9.8	A	FM; $S = 4$	9d
UYOJIC[c]	100.8–99.7	98.8–95.5	4.4–5.4	10.5–10.8	A	FM; $S = 4$	9j
IROHIH[c]	99.7–98.9	99.6–95.8	5.9–7.3	9.2–9.8	A	FM; $S = 4$	9i
FADTOV[b]	100.5	98.6; 96.7	5.6	10.7	A	FM; $S = 4$	9g
	98.7	99.5–98.1	9.1	9.3			
BEPBON[b]	99.8	98.2; 94.3	3.8	9.5–9.9	A	FM; $S = 4$	9b
	99.7	99.3; 93.3	3.5	9.9			
$[Ni_4(pym)_4(\mu\text{-}RCOO)_4]$							
CEDCEW[c]	102.6–102.2	96.1–92.7	3.9–2.2	12.9–12.2	A	AF; FM; $S = 0$	9o
CEDCIA[c]	103.5–102.7	95.2–91.3	4.7–4.3	14.4–11.9	A	AF; FM; $S = 0$	9o
CEDCOG[c]	103.4–103.2	93.7–91.6	6.8–6.2	13.4–13.3	A	AF; FM; $S = 0$	9o
DOWRAK	102.2	95.5; 92.9	2.5	12.2	A	AF; FM; $S = 0$	9m
LEZXIZ	102.7	92.7; 95.4	3.2	12.7	A	AF; FM; $S = 0$	9l
$[Ni_4(pym)_4(\mu\text{-}RCOO)_2X_2S_2]$							
SIYSID[b,c]	99.6–99.1	101.3–101.9; 93.0–91.3	5.9–6.0	1.9–1.4; 17.5–17.2	B	AF; FM; $S = 0$	9f
	102.3–98.6	102.1–100.7; 92.3–91.5	4.7	2.4–1.7; 19.5–17.8			
TUFPEQ[c]	102.2; 100.0	101.5–100.1	1.8–1.3	2.2–0.9; 20.2–19.2	B	AF; FM; $S = 0$	12a
		90.7–88.9					

[a] CCDC code. [b] Complexes with two non-equivalent cubes in the unit cell. [c] All angles of the cube are different. The tabulated values correspond to the range between the larger and shorter angles.

493